Quality Checks and Validation Procedures for PPP-GNSS data analysis at INGV

Nicola D'Agostino

05/02/2018

ASSOCIATED PRODUCTS:

WP10-DDSS-07 Products.EPOS.PPPsolution

WP10-DDSS-09 Products.EPOS.PPPsolution.TS

WP10-DDSS-13 Products.EPOS.PPPsolution.velocity

INTRODUCTION

This document describes the quality checks and validation procedures performed at the EPOS WP10 INGV analysis center on the PPP (precise point positioning) daily solutions and the associated results. The processing strategy and the reference alignment are briefly described for the understanding of the quality check and validation procedures.

INPUT FILES AND METADATA

The ppp solutions, obtained using the software package Gipsy, include the EPOS WP10 prototype network composed of stations from the EUREF, IGS, NOA, RENAG and RING (Avallone et al. 2010) networks (Figure 1) in the time interval 2000-2017. Metadata for the selected stations have been extracted from the file following sources:

Network	Metadata
EUREF	ftp://epncb.oma.be/pub/station/general/euref.snx
RING	IGS log files from: ftp://gpsfree.gm.ingv.it/SITELOG/LOGFILE/RING/
RENAG	Sinex file extracted from: RENAG GNSS GSAC Repository (http://epos.unice.fr:8080/renagbgsac)
NOA	Sinex file extracted from: http://194.177.194.238:8080/noanetgsac/gsacapi/
IGS	ftp://ftp.igs.org/pub/station/general/igs.snx

PROCESSING STRATEGY

GPS data are reduced using the Jet Propulsion Laboratory (JPL) GIPSY-OASIS II software (ver.6.3) in a Precise Point Positioning mode (Zumberge et al., 1997) applied to ionospheric-free carrier phase and pseudorange data and using JPL's final fiducial-free GPS orbit products. We apply the VMF1 grids tropospheric mapping function (Boehm et al., 2006) and estimate tropospheric wet zenith delay and horizontal gradients as stochastic random-walk parameters every 5 min (Bar-Sever et al., 1998), to model tropospheric refractivity. We compute the ocean loading from the FES2004 tidal model coefficients provided by the Ocean Tide Loading Provider (http://holt.oso.chalmers.se/loading) and apply it as a station motion model (Scherneck et al., 1991). Ambiguity resolution is applied using the wide lane and phase bias (WLPB) method (Bertiger et al., 2010). In order to to reduce the common mode signal, we relaized a terrestrial reference frame (named EU17) for crustal deformation studies following the approach described in Blewitt et al.(2013) and in Métois *et al.(2015)*. This frame is defined by 6 Cartesian coordinates and velocities for 132 stations selected by specific quality criteria (FRAME stations in Figure 1). These criteria include the time interval of observation, a minimum number of antenna changes, reduced amplitude of periodic signals, and linear behavior. Our realization of the reference frame is aligned in origin and scale with IGS08 (Rebishung et al., 2008). In a complementary version is also implemented to have no-net rotation with respect to the stable interior of the Eurasian plate, realized by minimizing the horizontal velocities of a 32-stations core subset (Eu Core Figure 1). This version allows the alignment in an “Eurasian” frame and to obtain time series that are directly in the Eurasian reference frame. To allow combinations with additional daily solutions, the ppp daily solutions are also provided with a “loosened” covariance matrix with large variances in the 7 transformation parameters and using procedure described by Blewitt (1998). This covariance augmentation is accomplished using the GIPSY “staproject-u” command. The resulting full covariance matrix is then suitable to invert into a full weight matrix to be used for a global fit to all station epoch positions and velocities in one step. To summarize the following table provides a synoptic view of the products:

Id	Description
INGwwwwd.block.snx.Z	PPP solutions in IGS08b. Diagonal covariance matrix (no correlation between stations).
INGwwwwd.loose.snx.Z	PPP solutions in IGS08b. Loosened covariance matrix.
INGwwwwd.Eu.block.snx.Z	PPP solutions in IGS08b rotated to have a no-net rotation of the “stable” part of the Eurasia plate. Diagonal covariance matrix (no correlation between stations).

QUALITY CHECKS AND VALIDATION OF REFERENCE FRAME ALIGNMENT

The number of stations (Figure 2) used every day for the alignment to the EU17 refence frame increases linearly from 2000 to 2008, it then remains stable at 110-130 stations between 2008 and 2016, and starts to decrease after 2016. As stations fail, equipment is replaced, and large earthquakes occur, the number of contributing frame stations naturally tends to decrease with time. This factor, together with increasing extrapolation error in the predicted position of frame stations with time, implies that the reference frame starts to degrade and it became obsolete after some time. Potential improvements warrants further efforts to find the best combination of stations as to make the number and geometry of contributing as stable as possible. The WRMS (weighted-root-mean-squares) time serie of the residuals of the FRAME stations used for frame alignment is show in Figure 2. Average WRMS value are 1.2, 1.0 and 3.7 mm for the North, East, and Up components, respectively. These values, together with the number of contributing stations, are used to evaluate the quality of the daily alignments. The 7 Helmert transformation parameters deriving from this trasformation are shown in Figure 3.

QUALITY CHECKS AND DATA CLEANING OF TIME SERIES

To evaluate the daily dispersion of the daily coordinates, residuals are calculated in a NEU (North, East, Up) system with respect to an estimate of linear velocity with annual and semiannual periodic signals obtained using the CATS software (Williams, 2007). This first velocity estimate is obtained assuming a white noise model of the covariance matrix of the data. Epochs of offset are given as a-priori input values to the CATS software and include time of antenna change and significant seismic events. Each position time series was cleaned using a robust outlier detection algorithm (Nikolaidis, 2002) applied to postfit residuals. The cleaning algorithm is based on the median and the interquartile range (IQR) statistics to describe the central value and spread of the data. The IQR of a data sample is the difference between its 75th and 25th percentiles. The median and IQR are computed within a sliding window centered on each daily measurement. The outliers are defined as having an absolute value of their difference relative to the median larger than 3 time the IQR, where the window size is 1 year. For each site, outlier epochs are identified separately in each coordinate direction and then applied to all three coordinates directions. With this edit criterion, the cleaning algorithm removes 11±3% of the data points (on 615 stations). Figure 4 and 5 show the effects of the data cleaning on a station characterized by a very stable behavior (TREM) and on a station characterized by significant annual and multi-annual periodicties (MCRV). It can be observed that the use of a sliding window allows the detection of outliers also for time series (MCRV Figure 5) characterized by natural (see Silverii et al., 2016) annual and multi-annual hydrological signals. After data cleaning the final velocity estimate and associated uncertainties are obtained using CATS assuming a flicker-noise model of the covariance matrix of the data. The effect of data cleaning can be observed in Figure 6 with discrete (top 6 plots) and cumulative histogram distributions (bottom 6 plots). The effect of data cleaning is to eliminate outliers in the WRMS distibutions and to significantly decrease the median of WRMS distributions in all the three components.

QUALITY CHECKS AND VALIDATION OF STATION VELOCITIES

GPS velocities and related uncertainties are also obtained using the robust trend estimator MIDAS (Blewitt et al., 2016). The MIDAS-estimated velocity is essentially the median of the distribution of values calculated using pairs of data in the time series separated by approximately 1 year, making it insensitive to seasonal variation and time series outliers. Additional tests also shows that MIDAS is relatively insenstitive to the presence of antenna offsets which clearly stand out in the probability density function of velocity pairs. MIDAS provides uncertainties based on the scaled median of absolute deviations of the residual dispersion. The uncertainties have been shown to be realistic by Blewitt et al. (2016) and do not require further scaling. Figure 7 display the estimated standard deviations by CATS (flicker noise) and MIDAS as a function of the observation interval. Figure 7 also displays a comparison between the CATS (flicker noise model) and the MIDAS uncertainty estimates showing that the large majority of the velocities differ by less than ±1 mm/yr .

References

Avallone, A. *et al.* The RING network: improvements to a GPS velocity field in the central Mediterranean. *Ann. Geophys.* **53**, 39-54 (2010).

Bar-Sever, Y. E., Kroger, P. M. & Borjesson, J. A. Estimating horizontal gradients of tropospheric path delay with a single GPS receiver. *J. Geophys. Res.* **103**, 5019-5025 (1998).

Bertiger, W. *et al.* Single receiver phase ambiguity resolution with GPS data. *J. Geod.* **84,** 327-337 (2010).

Blewitt, G., C. Kreemer, W. C. Hammond, and J. M. Goldfarb (2013), Terrestrial reference frame NA12 for crustal deformation studies in North America, *J. Geodyn.*, *72*, 11–24.

Blewitt, G., Kreemer, C., Hammond, W. C. & Gazeaux, J. MIDAS robust trend estimator for accurate GPS station velocities without step detection. *J. Geophys. Res.* **121**, 2054-2068 (2016).

Boehm, J. Werl, B. & Schuh, H. Troposphere mapping functions for GPS and very long baseline interferometry from European Centre for Medium-Range Weather Forecasts operational analysis data. *J. Geophys. Res.* **111**, B02406, 10.1029/2005JB003629 (2006).

Métois, M. *et al.* Insights on continental collisional processes from GPS data: Dynamics of the peri-Adriatic belts. *J. Geophys. Res.* **120**, 8701-8719 (2015).

Nikolaidis, R. Observation of Geodetic and Seismic deformation with the Global Positioning System, PhD Thesis, University of California San Diego.

Rebischung, P. *et al.* IGS08: The IGS realization of ITRF2008. *GPS Sol.* **16**, 483-494 (2012).

Scherneck, H. A parametrized solid earth tide model and ocean tide loading effects for global geodetic baseline measurements. *Geophys. J. Int.* **106**, 677-694 (1991).

Williams, S. D. P. (2007), CATS: GPS coordinate time series analysis soft- ware, GPS Solutions, 12, 147–153, doi:10.1007/s10291-007-0086-4.

Zumberge, J. F., Heflin, M. B., Jefferson, D. C., Watkins, M. M. & Webb, F. H. Precise point positioning for the efficient and robust analysis of GPS data from large networks. *J. Geophys. Res.* **102,** 5005-5017 (1997).

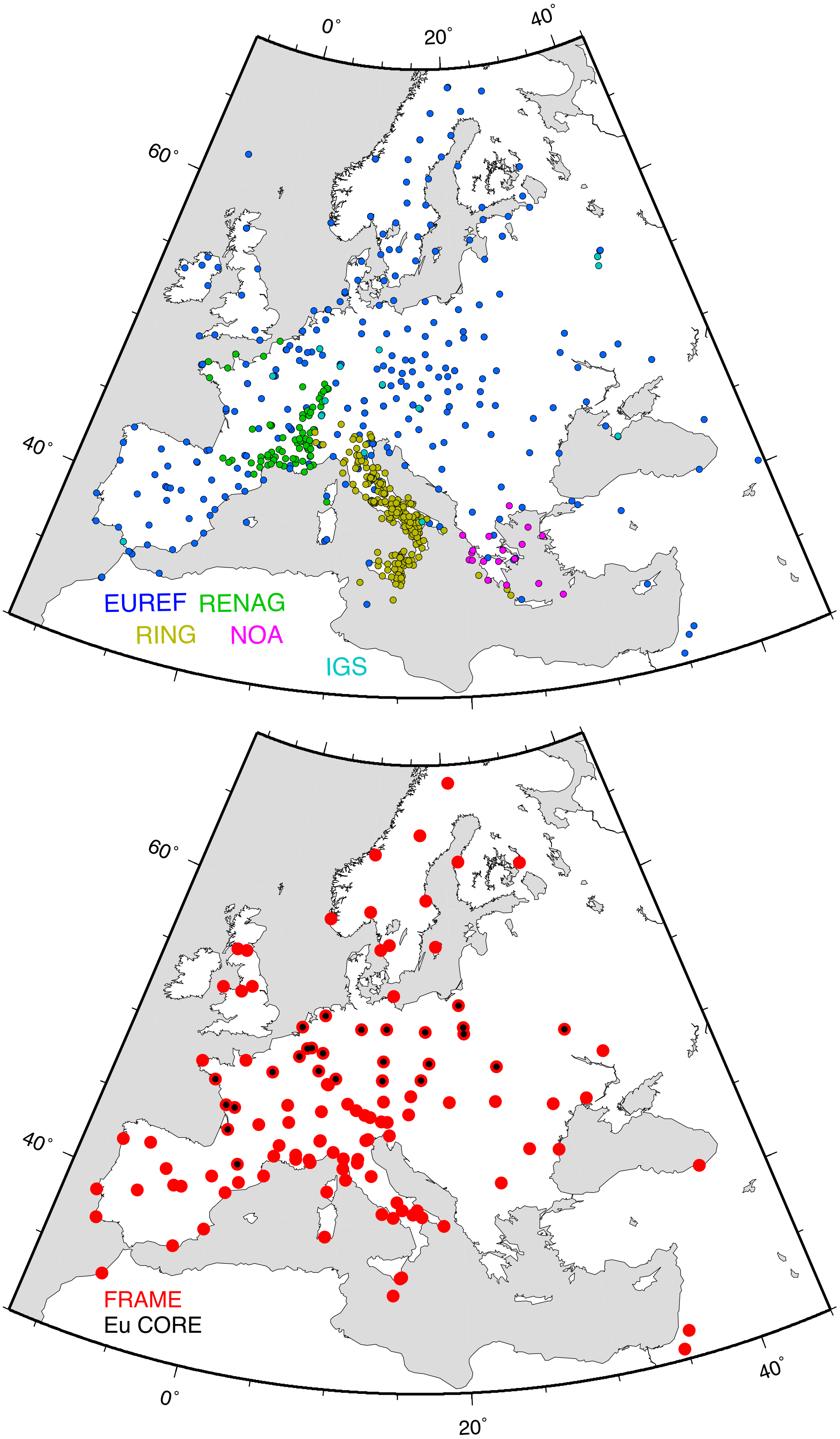

Figure 1

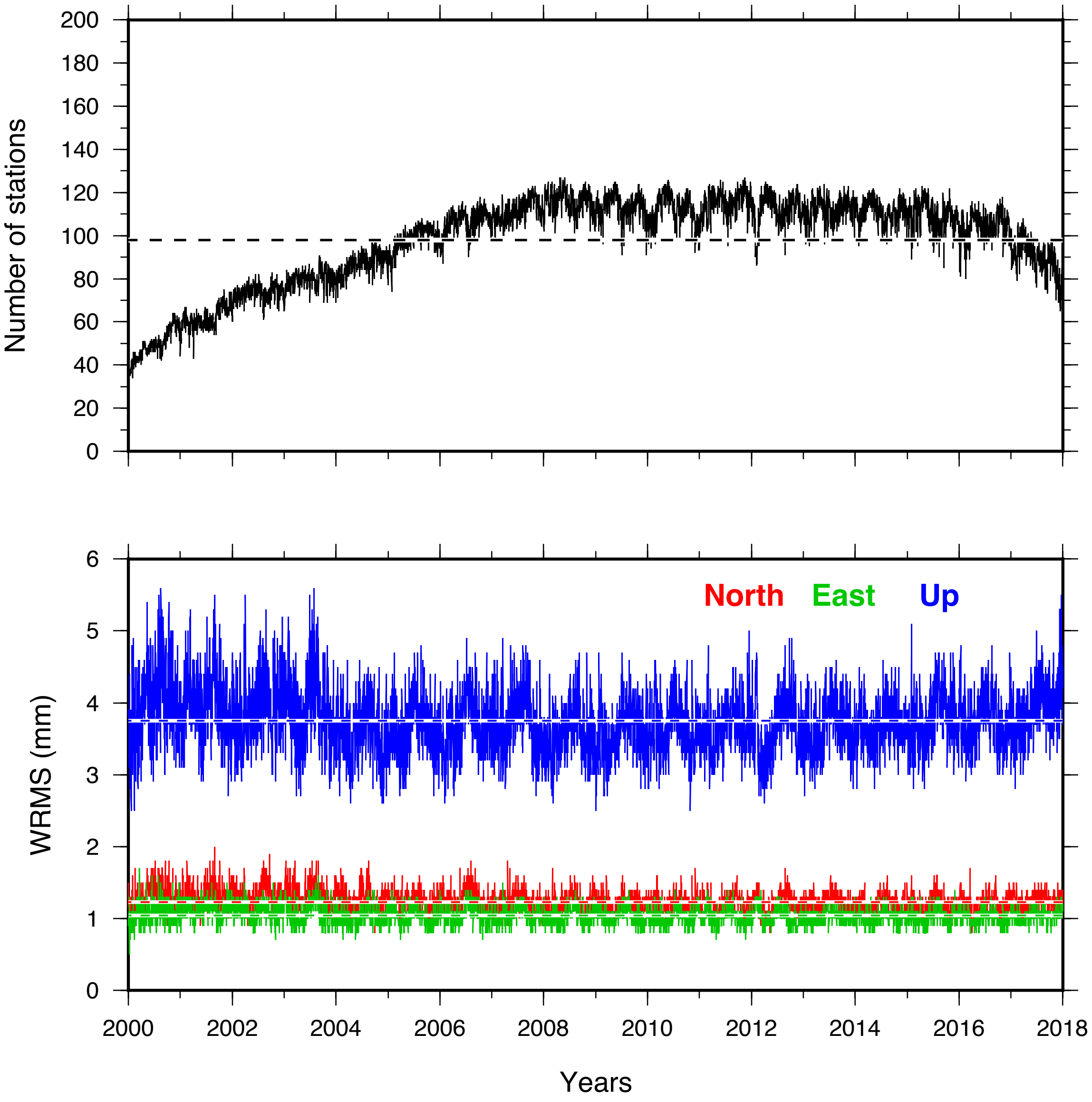
200
180
160
140
120
100
80
60
40
20
0
Number of stations
6
5
4
3
2
1
0
WRMS (mm)
North
East
Up
2000
2002
2004
2006
2008
2010
2012
2014
2016
2018
Years

Figure 2

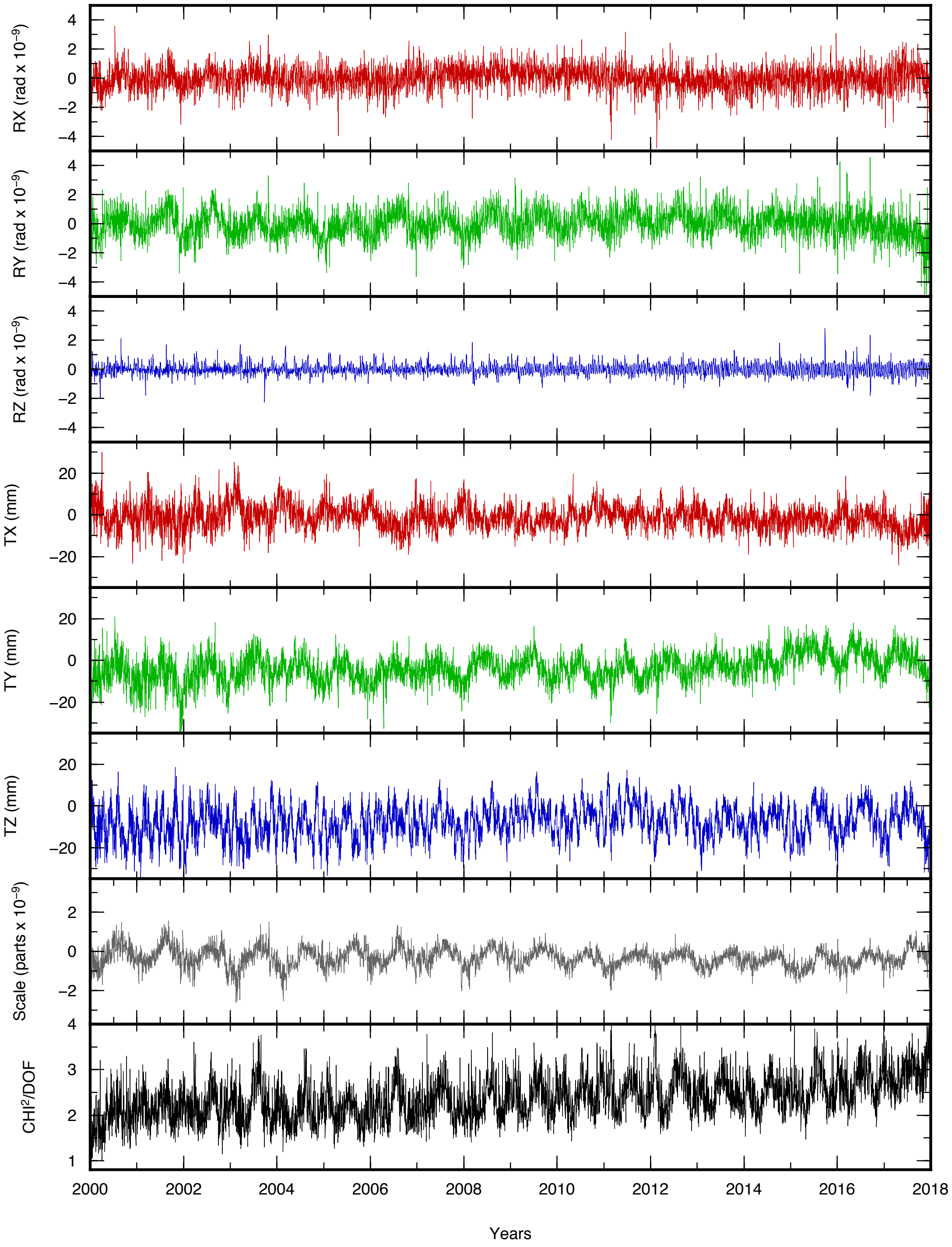
RX (rad x 10^{-9})
4
2
0
−2
−4
RY (rad x 10^{-9})
4
2
0
−2
−4
RZ (rad x 10^{-9})
4
2
0
−2
−4
TX (mm)
20
0
−20
TY (mm)
20
0
−20
TZ (mm)
20
0
−20
Scale (parts x 10^{-9})
2
0
−2
CHI^2/DOF
4
3
2
1
2000
2002
2004
2006
2008
2010
2012
2014
2016
2018
Years

Figure 3

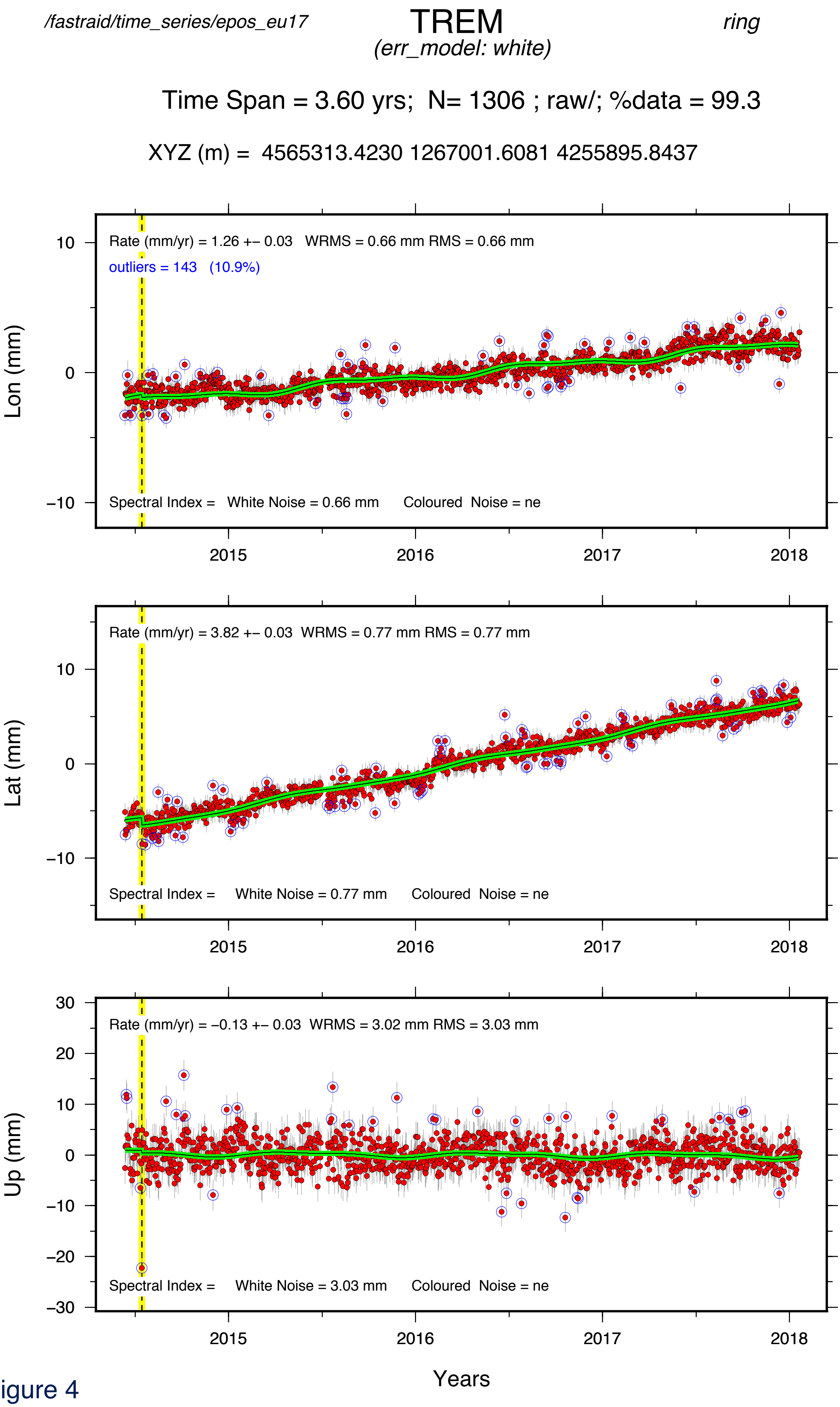
/fastraid/time_series/epos_eu17
TREM
ring
(err_model: white)
Time Span = 3.60 yrs; N= 1306 ; raw/; %data = 99.3
XYZ (m) = 4565313.4230 1267001.6081 4255895.8437
Rate (mm/yr) = 1.26 +– 0.03   WRMS = 0.66 mm RMS = 0.66 mm
outliers = 143   (10.9%)
Spectral Index =   White Noise = 0.66 mm   Coloured Noise = ne
Lon (mm)
10
0
–10
2015
2016
2017
2018
Rate (mm/yr) = 3.82 +– 0.03 WRMS = 0.77 mm RMS = 0.77 mm
Spectral Index =   White Noise = 0.77 mm   Coloured Noise = ne
Lat (mm)
10
0
–10
2015
2016
2017
2018
Rate (mm/yr) = –0.13 +– 0.03 WRMS = 3.02 mm RMS = 3.03 mm
Spectral Index =   White Noise = 3.03 mm   Coloured Noise = ne
Up (mm)
30
20
10
0
–10
–20
–30
2015
2016
2017
2018
Years

Figure 4

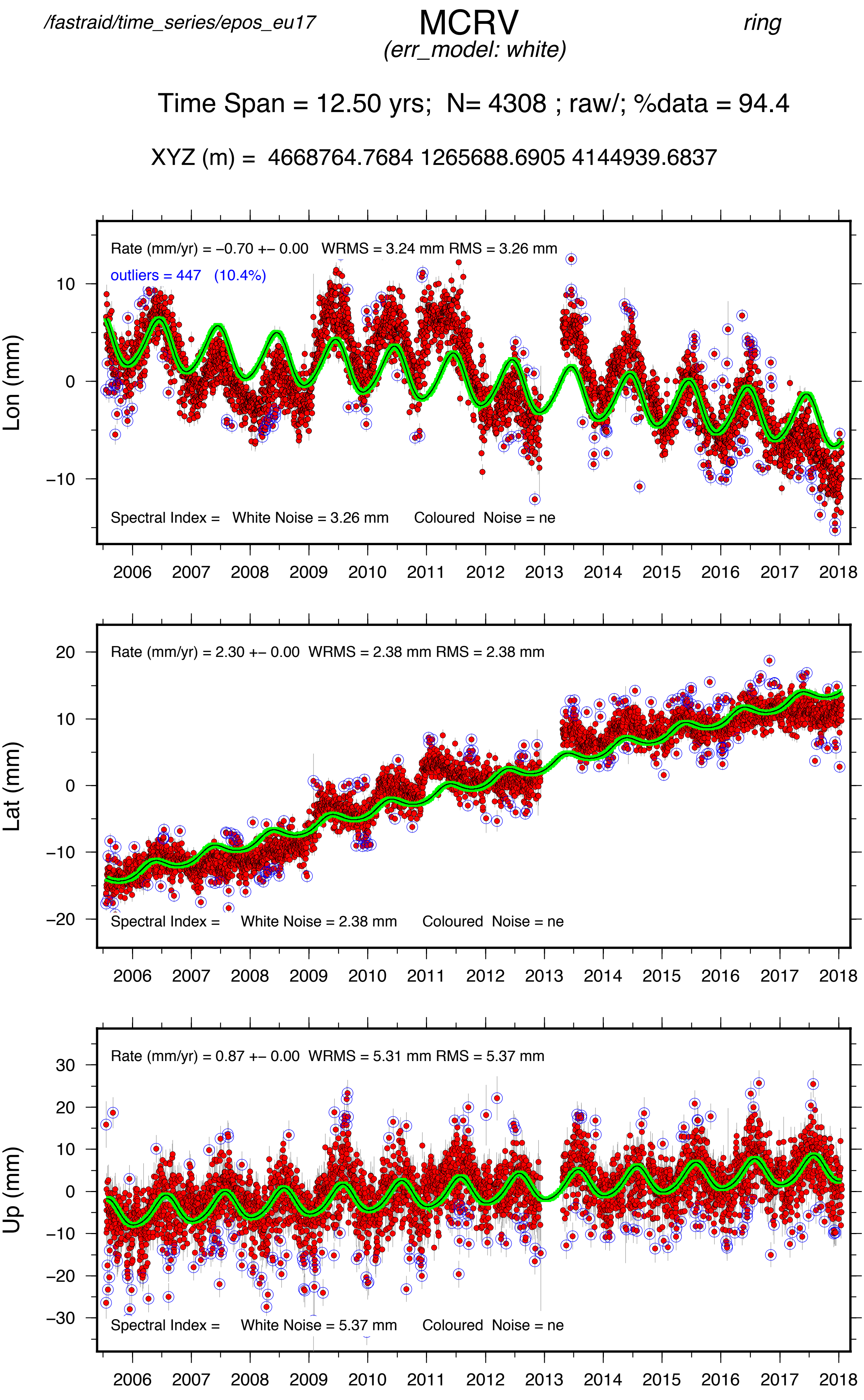
/fastraid/time_series/epos_eu17
MCRV
(err_model: white)
ring
Time Span = 12.50 yrs; N= 4308 ; raw/; %data = 94.4
XYZ (m) = 4668764.7684 1265688.6905 4144939.6837
Rate (mm/yr) = –0.70 +– 0.00   WRMS = 3.24 mm RMS = 3.26 mm
outliers = 447   (10.4%)
Spectral Index =   White Noise = 3.26 mm   Coloured Noise = ne
Lon (mm)
10
0
–10
2006
2007
2008
2009
2010
2011
2012
2013
2014
2015
2016
2017
2018
Rate (mm/yr) = 2.30 +– 0.00 WRMS = 2.38 mm RMS = 2.38 mm
Spectral Index =   White Noise = 2.38 mm   Coloured Noise = ne
Lat (mm)
20
10
0
–10
–20
2006
2007
2008
2009
2010
2011
2012
2013
2014
2015
2016
2017
2018
Rate (mm/yr) = 0.87 +– 0.00 WRMS = 5.31 mm RMS = 5.37 mm
Spectral Index =   White Noise = 5.37 mm   Coloured Noise = ne
Up (mm)
30
20
10
0
–10
–20
–30
2006
2007
2008
2009
2010
2011
2012
2013
2014
2015
2016
2017
2018

Figure 5

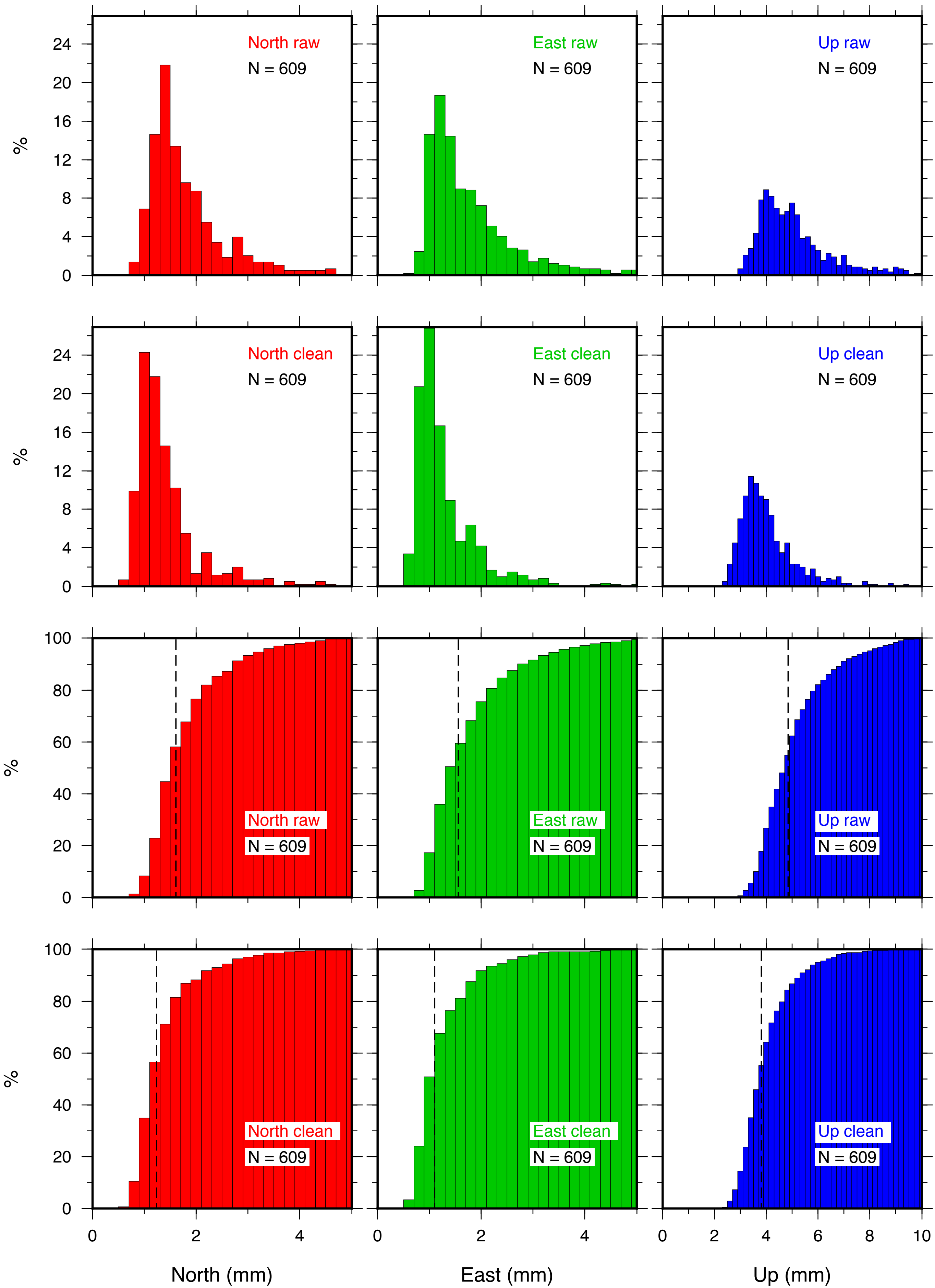

North raw
N = 609
East raw
N = 609
Up raw
N = 609
North clean
N = 609
East clean
N = 609
Up clean
N = 609
North raw
N = 609
East raw
N = 609
Up raw
N = 609
North clean
N = 609
East clean
N = 609
Up clean
N = 609
%
0
4
8
12
16
20
24
0
20
40
60
80
100
0
2
4
0
2
4
0
2
4
6
8
10
North (mm)
East (mm)
Up (mm)

Figure 6

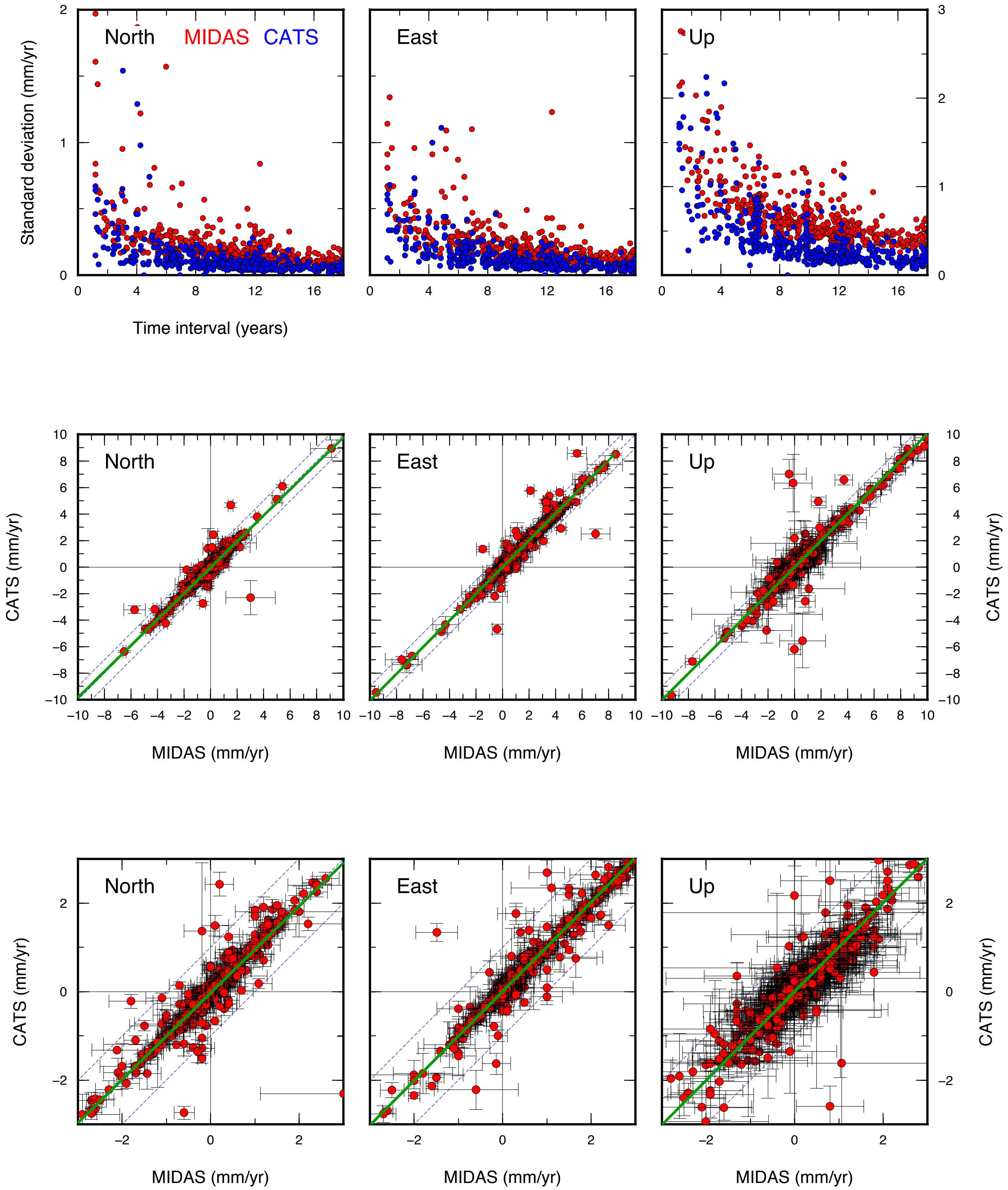
North
MIDAS
CATS
East
Up
Standard deviation (mm/yr)
Time interval (years)
0
4
8
12
16
0
1
2
3
CATS (mm/yr)
MIDAS (mm/yr)
−10
−8
−6
−4
−2
0
2
4
6
8
10

Figure 7